

# HOW THE REVERSAL OF THE MAGNETIC FIELD OF THE SUN MODULATES SNOWFALL IN THE SIERRA NEVADA MOUNTAIN RANGE OF THE WESTERN UNITED STATES.

John A. Kleppe<sup>1\*</sup> and Daniel S. Brothers<sup>2</sup>

## ABSTRACT

We have shown in previous papers the major driving forces of winter precipitation, in the form of snow, in the Sierra, Cascade, and Rocky mountain ranges are the reversal of the sun's magnetic field and a statistically-independent "carrier" signal being generated by the Earth's large-scale atmospheric circulation parameters. In this paper we present the mechanism by which our proposed Sun-Earth magnetic carrier suppressed amplitude modulation system modulates the formation of the Sierra snowpack resulting in the generation of signals detected in the SWE records. We show how solar magnetic activity affects atmospheric circulation in the western tropical Pacific including the connections, between the El Nino-Southern Oscillation, the Walker circulation, and the resulting variability in the lower thermosphere. A combined solar and geomagnetic index for thermospheric climate is used along with wavelet analysis to explain how the reversal of the sun's magnetic field modulates the Sierra mountain snowpack. The results of this work will provide a very useful basis for studying drought patterns related to the magnetic activity of the sun. (KEYWORDS: solar magnetic reversal, snow water equivalent, El Nino)

## INTRODUCTION

Snowpack in the Sierra mountain range, located in the western United States, provides a natural form of water storage which greatly impacts the economies of the region. (Kleppe & Brothers, 2017, 2018) concluded the major driving forces of winter precipitation, in the form of snow, in the northern and central Sierra are the reversal of the sun's magnetic field; and, a statistically independent "carrier" signal being generated by the Earth's atmospheric circulation. The snowpack variability in the Sierra is not only a function of individual watersheds and/or local topographic relief, but is to a larger degree, a function of broad-scale climatic phenomena affecting the entire Sierra Nevada mountain range. The El Nino Southern Oscillation (ENSO) (Figure 1) is one of the most important ocean/atmospheric interactions that produce the snowpack variability in the Sierra. During an El Nino event, the surface waters in the central and eastern Pacific Ocean become significantly warmer than usual. That change is intimately tied to the atmosphere and to the winds blowing over the vast Pacific. Easterly trade winds (which blow from the Americas toward Asia) falter and can even turn around into westerlies. This allows great masses of warm water to slosh from the western Pacific toward the Americas. It also reduces the upwelling of cooler, nutrient rich waters from the deep thus shutting down or reversing ocean currents along the equator and along the west coast of South and Central America.

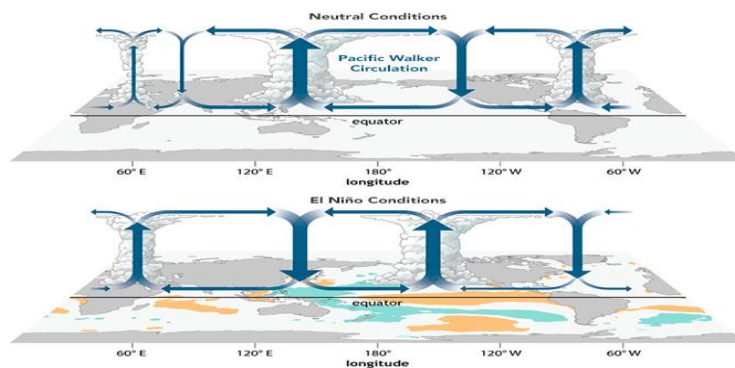


Figure 1. Atmospheric circulation over the equator, the Walker circulation, changes substantially with the arrival of El Nino. (Illustration by NOAA/Climate.gov).

Paper presented Western Snow Conference 2019

<sup>1</sup>John A. Kleppe, College of Engineering, University of Nevada, Reno, Reno, NV 89557, [Kleppe@unr.edu](mailto:Kleppe@unr.edu)

<sup>2</sup>Daniel S. Brothers, Pacific Coastal and Marine Science Center, U.S. Geological Survey, Santa Cruz, CA.95060

The circulation of the air above the tropical Pacific Ocean responds to this redistribution of ocean heat. The typically strong high-pressure systems of the eastern Pacific weaken, thus changing the balance of atmospheric pressure across the eastern, central, and western Pacific. While easterly winds tend to be dry and steady, Pacific westerlies tend to come in bursts of warmer, moister air, from <https://earthobservatory.nasa.gov/features/ElNino>.

The Oceanic Niño Index (ONI) [3 month running mean of ERSST.v5 SST anomalies in the Niño 3.4 region (120°W-170°W, 5°N-5°S)], is based on centered 30-year base periods updated every 5 years. The ONI index has become the de-facto standard that NOAA uses for identifying El Niño (warm) and La Niña (cool) events in the tropical Pacific. The ONI index is one of the oldest indices for monitoring ENSO and is defined as:

$$\text{ONI} = \text{SSTA}_{(120^{\circ}\text{W}-170^{\circ}\text{W}, 5^{\circ}\text{S}-5^{\circ}\text{N})} \quad [1]$$

The EMI (Modoki) index is also an index of SST anomalies averaged over three areas of the tropical Pacific Ocean. The Modoki mode is associated with strong anomalous warming in the Central tropical Pacific and cooling in the Eastern and Western tropical Pacific. The EMI captures the zonal pattern of the Modoki mode and is defined in [Ashok et al., 2007]:

$$\text{EMI} = \text{SSTA}_{(165^{\circ}\text{E}-140^{\circ}\text{W}, 10^{\circ}\text{S}-10^{\circ}\text{N})} - 0.5\text{SSTA}_{(110^{\circ}\text{W}-70^{\circ}\text{W}, 15^{\circ}\text{S}-5^{\circ}\text{N})} - 0.5\text{SSTA}_{(125^{\circ}\text{E}-145^{\circ}\text{E}, 10^{\circ}\text{S}-20^{\circ}\text{N})} \quad [2]$$

### **Simplified Model of the Sun**

The sun, as a simplified model, can essentially be described as a sphere of rotating plasma; and because the equator of the sun is rotating faster than at the poles, magnetic flux lines are "pulled" around and stretched by the rotational difference. As the sun continues to rotate the magnetic lines are twisted into toroids and magnetically induced currents in the sun begin to flow. The flowing currents produce temperature differences we observe as sunspots. When the sunspot activity reaches a maximum of activity (minimal magnetic strength) the sun reverses its magnetic field. The resulting reverse currents cause a reduction of the total current flow and the number of sunspots begins to decrease with the sunspots retaining their magnetic polarity. The currents and the resulting sunspots approach zero and the sun is once again at its maximum magnetic field strength but with a reversed magnetic polarity. The sun reverses its entire magnetic field every solar cycle of approximately 11 years and then reverses again to return to its original magnetic state after the following solar cycle. The induced currents caused by the changing magnetic field are directly proportional to the magnitude of the magnetic field and inversely proportional to the duration of the reversal.

## **DATA AND METHODOLOGY**

### **Spectral Analysis**

Among all the spectral analysis tools used in frequency analysis, the most commonly applied is the Fourier transform. Although the Fourier transform is efficient and robust for analyzing the frequency content of a periodic signal over an entire time record, it is limited in its ability to detect changes in frequency as a function of time. The Morlet Wavelet transform, on the other hand, can capture the short duration, high frequency, as well as the long duration, low frequency information simultaneously.

We investigated using Morlet wavelets, several long-term snow water equivalent (SWE) records in the northern and central Sierra Nevada and found non-linear linkages between sunspots or 10.7cm data (i.e., the magnetic activity of the sun) and SWE, (Kleppe & Brothers, 2017). We later extended our work (Kleppe & Brothers, 2018) to include SWE records located in the southern Sierra, Rocky, and Cascade mountains.

It is important to note the 11 year and 22-year visible sunspot cycles are **NOT** found in the SWE data, but rather, we found evidence of a non-linear Sun-Earth magnetic carrier suppressed amplitude modulation system resulting in the generation of four signals that modulate the formation of the Sierra snowpack. Researchers continue to search for the connection between the variability of the sun and that of the Earth's troposphere to the point it has become "third-rail science", (Zhai, 2017), (Leamon et al., 2018). The main problem has been the scientific community continues to attempt to directly correlate Earth's climate with the 11 and/or 22-year solar cycles.

## **RESULTS**

We investigated, using our model, the running 3-month mean sea surface temperature ONI data available for El Niño in the Niño 3.4 region i.e., equation [1]. Figure 2 shows the Morlet wavelet spectral content of the ONI converted to Water Year (WY) for the period WY 1951 to WY 2017.

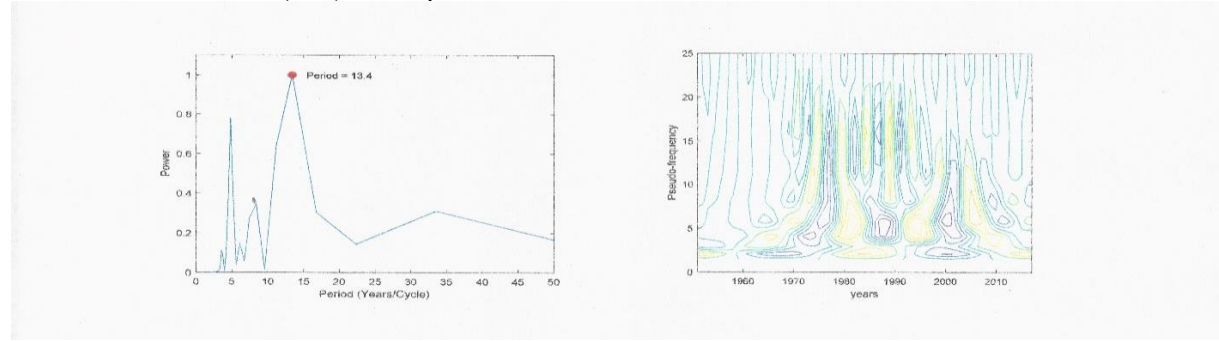


Figure 2. Wavelet spectral record of the Oceanic Niño Index (ONI) from WY 1951 to WY 2017

The four spectral peaks due to the reversal of the magnet field of the sun are found to be at periods  $T_1 = 6.0909$ ,  $T_2 = 8.375$ ,  $T_3 = 13.4$ , and  $T_4 = 33.5$ . These periods are shown as equation [3], (Kleppe & Brothers, 2017, 2018). The  $T_n$  are the respective periods calculated as the inverses of each  $f_n$ :

$$\begin{aligned} f_{1=1/T_1} &= f_c + f_s + f_g = 1/6.0909 = 0.164190 \\ f_{2=1/T_2} &= f_c + f_s - f_g = 1/8.3750 = 0.119403 \\ f_{3=1/T_3} &= f_c - f_s + f_g = 1/13.400 = 0.074629 \\ f_{4=1/T_4} &= f_c - f_s - f_g = 1/33.500 = 0.029851 \end{aligned} \quad [3]$$

The unique solution for this set of simultaneous equations is found to be:  $f_c = 0.09702$  or  $T_c = 10.31$  years,  $f_s = 0.04478$  or  $T_s = 22.33$  years, and  $f_g = 0.022389$  or  $T_g = 44.67$  years. It can be shown that  $T_s = 22.33$  years is the average of the solar cycles over the period of WY1951 to WY2017, and  $T_g$  is the average of the Gleissberg Cycle over the same period WY 1951 to WY 2017.

It is beyond chance that these spectral peaks in the ONI data match our proposed carrier suppressed AM modulation model. The other two spectral peaks,  $T_5 = 3.526$  years and  $T_6 = 4.7857$  years, also shown in Figure 2., are not due to the reversal of the magnetic field of the sun but are generated by redistribution of heat energy by ocean currents and atmospheric circulation, (Pinker, et al., 2017; Leamon et al., 2018). This is supported by researchers who have studied the "bleaching" of coral in the geographical area of the El Niño by using a band-pass filter to pass all 2 to 7-year periods over the past 7,000 years, (Cobb et al., 2013). The SST in this period band is time varying because the band includes the period  $T_1 = 6.0909$  years from the magnetic reversal of the sun discussed above. The authors also reported Twentieth-century ENSO variance is significantly higher than average fossil coral ENSO variance over the past 7,000 years but it is not unprecedented. They concluded that forced changes in ENSO, whether natural or anthropogenic, may be difficult to detect against a background of large internal variability.

## **DISCUSSION AND CONCLUSIONS**

The Thermosphere Climate Indexes (TCI) represent the 60-day running average of the global infrared cooling radiated from the thermosphere by nitric oxide and by carbon dioxide. The TCI are accurately expressed as linear combinations of the 60-day running averages of the F10.7cm data (sunspot cycles), (Mlynczak et al., 2018). The TCI directly links solar activity to the average temperature of the thermosphere; however, the energy change is so small, compared to the earth's energy budget, it is impossible to modulate the earth's energy balance, private communications (Mlynczak, 2019).

However, at the end of each solar cycle when the induced currents reverse direction the magnetic field strength of the sun bursts to a maximum and creates a "terminator". These terminators have been reported to have a strong correlation between solar and tropospheric variability. The swings from El Niño to La Niña are related to the phase of the solar cycle's "fiducial clock" that resets when the sunspots are gone from the solar disk. The rapidity of the response of cloud patterns to changing GCR flux indicate that denser clouds shift some 30°E within a month, one

month after the drop in cosmic rays. While the exact mechanism remains to be elucidated, changes in cosmic ray flux appear to be the driver of these ENSO swings (Leamon et al., 2018).

The modulation of the SST by the reversal of the magnetic field of the sun comes from the modulation of the downward short wave radiation flux, SW↓ and the downward long wave radiation flux, LW↓. The lag-correlation coefficients between EMI and SW↓ and LW↓ have recently been reported by Pinker, et al. (2017). The SW↓ flux leads the EMI index by 1 month; and, the long wave radiation flux LW↓ also leads the EMI index by 1 month. It is important to note the time series of the radiative fluxes are correlated with the time series of the El Niño and the EMI indicating both radiative flux variations have the same solar spectral peaks as shown in Figure 2.

Cosmic rays are also thought to affect cloud formation on Earth by creating condensation nuclei. The role of ionization in atmospheric processes by GCRs has been a controversial matter since it was first suggested fifty years ago. However, Yu and Luo (Yu and Luo, 2014) and Svensmark et al. (Svensmark et al., 2017) have recently provided additional support for the inferred linkages between cosmic rays and clouds on Earth. They propose the Sun's changing magnetic field has an influence on GCRs, with a stronger magnetic field deflecting more cosmic rays and a weaker one allowing more into the solar system.

It is very important to note the spectral shift of the major "drought buster" (El Niño) peak 13.4 years shown in Figure 2. This peak period shifted from 16 years to 12 years over the 91-year SWE data record from 1916 to 2007, (Kleppe & Brothers, 2017). This is a period shift of approximately 0.044 years per year being generated by the time variable Gleissberg Cycle. The average period between the El Niño peaks is therefore getting shorter meaning more frequent Atmospheric Rivers are to be expected during upcoming winters.

## **REFERENCES**

Ashok, et al. 2007. El Niño Modoki and its possible teleconnection. *Journal of Geophysical Research*, Vol. 112, 2-27.

Cobb, et al. 2013. Highly Variable El Niño-Southern Oscillation Throughout the Holocene. *Science* Vol. 339, 67-70.

Kleppe J.A., & D. S. Brothers. 2017. Solar forcing of drought detected in snowfall records of the central Sierra Nevada, Western United States. *Proceedings 85<sup>th</sup> Western Snow Conference*, 25-38.

Kleppe J.A., & D. S. Brothers. 2018. Detection of reversal of the magnetic field of the sun in snowfall records in the Sierra, Rocky, and Cascade mountain ranges of the western United States. *Proceedings 86<sup>th</sup> Western Snow Conference*, 77-87.

Leamon, et al. 2018. Termination of Solar Cycles and Correlated Tropospheric Variability. Submitted to *Journal of Geophysical Research-Space Physics*, arXiv:1812.02692v1 [astro-ph.SR] for this version)

Mlynczak, et al. 2018. Thermosphere climate indexes: Percentile ranges and adjectival descriptors. *Journal of Atmospheric and Solar-Terrestrial Physics*, Vol. 174 28-31.

Mlynczak, M.G. 2019. Private communications.

Pinker, et al. 2017. ENSO impact on surface radiative fluxes as observed from space. *Journal of Geophysical Research: Oceans*, 7880-7896

Svensmark, H. et al. 2017. Increased ionization supports growth of aerosols into cloud condensation nuclei, *Nature Communications*, 8:2199, 1-9.

YU, F. & G. Luo. 2014. Effect of solar variations on particle formation and cloud condensation nuclei. *Environmental Research Letters*, Vol. 9 No. 4, 1-7.

Zhai, Q. 2017. Evidence for the effect of sunspot activity on the El Niño/Southern Oscillation. *New Astronomy*, Vol. 52, 1-7.